Journal of Microwaves, Optoelectronics and Electromagnetic Applications, Vol. 23, No. 2, e2024281143 May 2024
DOI: https://dx.doi.org/10.1590/2179-10742024v23i2281143

Article

Wave Impedance Equivalent Circuit Model for Square Loop Frequency Selective Surfaces

Everaldo Faustino da C. Júnior[1], Paulo Henique da F. Silva[2], Alfredo Gomes Neto[3]
Group of Telecommunications and Applied Electromagnetism, GTEMA,
Federal Institute of Paraíba, João Pessoa, PB, Brazil.
faustinocjr@gmail.com, phdafs@gmail.com, alfredogomes@ifpb.edu.br

Abstract— The equivalent wave impedance circuit model (ECM-WI) is presented for the analysis of frequency selective surfaces (FSS). The development of the analytical model is based on homogenization theory, as well as analogies between wave theory and transmission line theory. The coplanar strip model and the concept of wave impedance are used to scale the Marcuvitz model for periodic strip gratings of conductive strips, as well as to consider the influence of the presence of a lossy dielectric substrate on the frequency response of the FSS. In particular, the model is applied to the analysis of square loop FSSs and considering the normal incidence. The results obtained are presented by comparing full-wave simulations for the two proposed models, obtaining average deviations in absolute values (%) of 2.11 and 0.38 for resonance frequency and 3.45 and 5.49 for bandwidth. The prototype manufactured in FR-4 obtained a deviation of 2.56% for resonance frequency and 2.79% for bandwidth.

Index Terms— Frequency selective surfaces, equivalent circuit models, wave impedance.

I. INTRODUCTION

The interest of researchers and design engineers in the analysis of frequency selective surfaces (FSS) is due to various applications as spatial filters or as components of other electromagnetic structures [1], [2]. Rigorous analysis of an FSS structure requires the use of a full-wave method (FWM). However, in the initial design phase of an FSS, it is convenient for the design engineer to use approximate models.

The equivalent circuit model (ECM) is one of the most used for approximate analysis of FSS. The application of ECM to FSS is based on the equivalent circuit representation of a periodic strip gratings given by Marcuvitz [3], being useful for the design of FSS with conventional elements: dipole, patch, Jerusalem cross , loops [4]-[6]. The square loop FSS is among the most used geometry because of its transmission properties. Its analysis is simplified from the decomposition of electromagnetic fields into propagation modes (TE and TM), as well as defining an equivalent homogeneous propagation medium for each inhomogeneous transmission structure [7]-[10].

In this paper, the equivalent circuit model is revisited. Based on a review of the available literature, the Marcuvitz model is scaled to apply the ECM to square loop FSS. The ECM approximate analysis of an FSS in the configuration superimposed on a dielectric layer presents satisfactory results, in particular, for thin dielectrics or with relative electric permittivity close to unity. The model

Brazilian Microwave and Optoelectronics Society-SBMO *received 05 Dec 2023; for review 06 Feb 2024; accepted 16 May 2024*
Brazilian Society of Electromagnetism-SBMag *ISSN 2179-1074*

DOI: https://dx.doi.org/10.1590/2179-10742024v23i2281143

improvement proposals allow the analysis and design of the transmission characteristics of a square loop FSS, in terms of resonance frequency and bandwidth, with greater accuracy, mainly for dielectric support substrates with higher values of electric permittivity, as well as thickness.

Section II presents the ECM formulations for oblique and normal incidence and a description of the approach used in developing the equivalent wave impedance circuit model (ECM-WI) formulation. The FSS impedance is obtained by scaling the Marcuvitz model with an effective wavelength and including the coplanar line model for capacitive susceptance. The concept of wave impedance is used to obtain: i) input impedance (of two homogeneous dielectric media) and effective wavelength; ii) equivalent impedance and frequency response of the FSS structure. Section III presents the comparative studies carried out between the ECM, improved equivalent circuit model (iECM) and ECM-WI models implemented for square loop FSS, as well as the results available in the literature, in addition to the ECM-WI result evaluated in relation to the experimental result of the FSS square loop prototype. Final considerations are made in section IV.

II. Equivalent circuit model

A. Periodic Strip Gratings

From previous works on the equivalent circuit representation of a periodic strip gratings [3], [11]-[13], the normalized immittances (inductive reactance and capacitive susceptance) for oblique incidence of the TE and TM modes, are given according to the equations (1)-(4).

$$X_{TE} = \omega L_{TE} = cos(\theta) \cdot F(p, w, \lambda, \theta) \tag{1}$$

$$B_{TE} = \omega C_{TE} = 4sec(\theta) \cdot F(p, g, \lambda, \theta) \tag{2}$$

$$X_{TM} = \omega L_{TM} = sec(\phi) \cdot F(p, w, \lambda, \phi) \tag{3}$$

$$B_{TM} = \omega C_{TM} = 4cos(\phi) \cdot F(p, g, \lambda, \phi) \tag{4}$$

The functions *F* and *G*, given by Marcuvitz for oblique incidence of the TE and TM modes, are according to equations (5)-(6). The *G* function is a correction factor; *p* is the periodicity, *w* is the strip width, *g* is the strip separation, Fig. 1; θ and ϕ are the incidence angles given by *k*; λ is the wavelength in free space; $q = (w, g)$ and $\varphi = (\theta, \phi)$ are dummy variables; C± are functions for TE and TM modes.

$$F(p, q, \lambda, \kappa) = \frac{p}{\lambda}\left[ln\left(csc\frac{\pi q}{2p}\right) + G(p, q, \lambda, \kappa)\right] \tag{5}$$

$$G(p, q, \lambda, \kappa) = \frac{1}{2}\frac{(1-\beta^2)^2\left[\left(1-\frac{\beta^2}{4}\right)(C_+ + C_-) + 4\beta^2 C_+ C_-\right]}{\left(1-\frac{\beta^2}{4}\right) + \beta^2\left(1+\frac{\beta^2}{2}-\frac{\beta^4}{8}\right)(C_+ + C_-) + 2\beta^6 C_+ C_-} \tag{6}$$

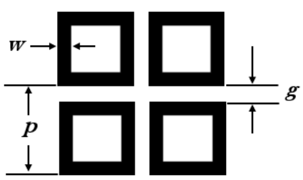

Fig. 1. Square loop FSS periodic arrangement.

This model presents better results for normal incidence [3], which is the most common application

  ISSN 2179-1074

from the design point of view. For normal incidence, it can be shown that the correction function *G* given in (6) can be rewritten in terms of Q and β according to the equations (7)-(9).

$$G(p,q,\lambda,\kappa) = \frac{Q}{1+Q\beta^4}(1-\beta^2)^2 \tag{7}$$

$$Q = C_+ = C_- = \left[1-\left(\frac{p}{\lambda}\right)^2\right]^{-1/2} - 1 \tag{8}$$

$$\beta = \sin\left(\frac{\pi q}{2p}\right) \tag{9}$$

For normal incidence, the equivalent circuit formulation for periodic strip gratings can be written as in (10)-(13). In this case, Marcuvitz hints at a simpler and more accurate expression for the correction factor *G*, rewritten in (13) in terms of Q and β, which is used in the equivalent circuit representation of a window formed by two obstacles in a rectangular waveguide with side view, Fig. 2(a), front view, Fig. 2(b) and equivalent circuit, Fig. 2(c).

$$X_{TE} = X_{TM} = \omega L = F(p,w,\lambda) \tag{10}$$

$$B_{TE} = B_{TM} = \omega C = 4F(p,g,\lambda) \tag{11}$$

$$F(p,q,\lambda) = \frac{p}{\lambda}\left[ln\left(csc\frac{\pi q}{2p}\right) + G(p,q,\lambda)\right] \tag{12}$$

$$G(p,q,\lambda) = (1-\beta^2)^2\left\{\left(\frac{Q}{1+Q\beta^4}\right)\left[\frac{p}{4\lambda}(1-3\beta^2)\right]^2\right\} \tag{13}$$

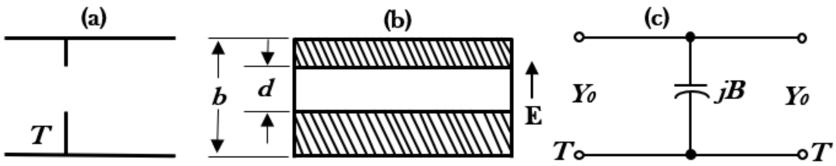

Fig. 2. Window in a rectangular waveguide: (a) side view; (b) front view; (c) equivalent circuit approximation.

B. Square Loop Frequency Selective Surface

The Marcuvitz model is widely used for approximate analysis of FSS. In the equivalent circuit models reported in the literature, for each type of FSS, the Marcuvitz model is scaled to obtain the values of normalized immittances for lumped components associated with the FSS structure. In particular, the geometric parameters of the periodic strip gratings (*w* and *g*) are scaled, as well as the *F* function given in (5). Some of these applications can be found in [10], [14]-[16]. The scattering problem from the normal incidence of electromagnetic radiation in a square loop FSS in the configuration superimposed on a supporting dielectric layer is illustrated in Fig. 3(a) and the associated equivalent circuit, in Fig. 3(b).

In this equivalent circuit model, a region of free space is represented as an infinite transmission line with the same characteristic wave impedance (Z_1=Z_3=Z_0) and FSS is represented by a shunt impedance (Z_{FSS}). The dielectric substrate layer of thickness (h) is represented by a section of transmission line of the same electrical length and impedance (Z_2).

  ISSN 2179-1074

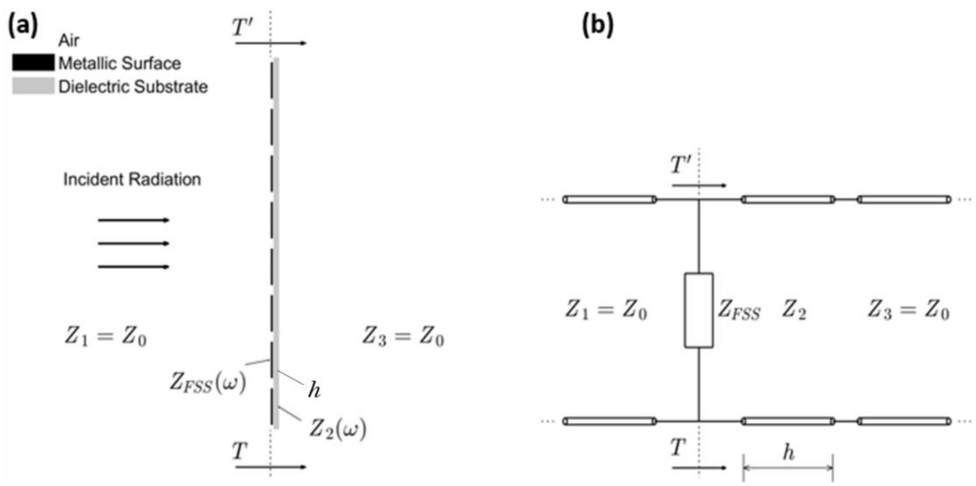

Fig. 3. FSS: (a) Representation of transmission in terms of impedances; (b) Equivalent circuit.

In the analysis of the transmission and reflection coefficients of an FSS using the ECM, the impedance of the dielectric substrate, the input impedance, the impedance of the FSS, and the equivalent impedance are considered.

The impedance of the lossy dielectric layer is calculated from the parameters of the non-magnetic material ($\mu_r = 1$): dielectric constant (ε_r) and loss tangent tg(δ), according to (14), [17].

$$Z_2 = \frac{Z_0}{\sqrt{\varepsilon_r[1 - jtg(\delta)]}} \tag{14}$$

The input impedance is calculated using the concept of wave impedance of an equivalent medium (in a three-medium problem, [17]) or equivalent LT (in a terminated LT problem, [18]), according to (15). Considering a dielectric substrate with small losses ($\text{tg}(\delta) < 0.1$, [17]; c=3×10^8 m/s), the propagation constant (γ) is given by (16), [10], [19].

$$Z_{in} = Z_2 \frac{Z_3 + Z_2 tanh(\gamma h)}{Z_2 + Z_3 tanh(\gamma h)} \tag{15}$$

$$\gamma = \omega\sqrt{\varepsilon_r}\left(\frac{\varepsilon_0 tg(\delta)}{2} Z_0 + j\frac{1}{c}\right) = \frac{\pi\sqrt{\varepsilon_r}}{\lambda}[tg(\delta) + j2] \tag{16}$$

After determining the input impedance, the scattering problem for FSS superimposed on a dielectric layer is shown in Fig. 4(a) and the associated equivalent circuit in Fig. 4(b). The condition $Z_{in} = Z_0$ corresponds to a freestanding FSS ($h = 0$), without a supporting dielectric layer.

In the ECM application for square loop FSS, the FSS impedance is modeled as the impedance of a band-stop RLC filter, as given in (17). Applications of ECM for square loop FSS are based on the following premise: the presence of the dielectric layer influences only the capacitive part of the FSS impedance [11], [20]. In this way, the Marcuvitz model [3], is scaled to calculate the normalized immittances, with q=2w and q=g, and multiplying (10) by the d/p factor and (11) by the $d/(p\varepsilon_{ref})$ factor, resulting in (18) and (19), respectively. The resistance associated with the FSS takes into account ohmic and dielectric losses (20), [10].

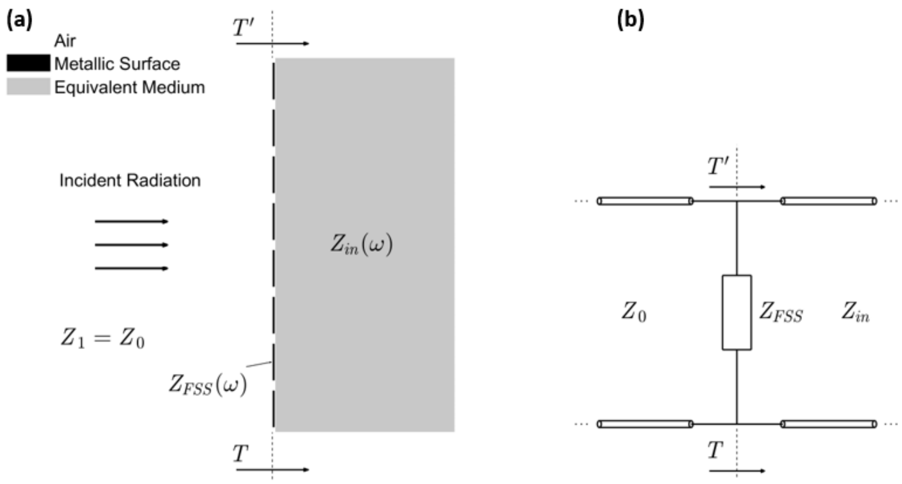

Fig. 4. FSS: (a) Illustration of the scattering problem in an FSS using the input impedance concept; (b) Equivalent circuit.

$$Z_{FSS}(\omega) = R_{FSS} + jZ_0(X_L - 1/B_C) \tag{17}$$

$$X_L = \omega L = \frac{d}{p} F(p, 2w, \lambda) \tag{18}$$

$$B_C = \omega C = 4\frac{d}{p}\varepsilon_{ref} F(p, g, \lambda) \tag{19}$$

$$R_{FSS} = R_\sigma + R_d = \sqrt{\frac{\omega\mu_0}{2\sigma}}\left(\frac{p^2}{2sd}\right) + \frac{tg(\delta)}{\omega C} \tag{20}$$

The effective electric permittivity of the square loop FSS in the overlapped configuration is given as a function of the thickness of the dielectric layer, h, according to (21), [10], [16]. In the limit $h \to \infty$, the effective permittivity tends to the asymptotic value, $(\varepsilon_r + 1)/2$.

$$\varepsilon_{ref} = \frac{(\varepsilon_r + 1)}{2} - \frac{(\varepsilon_r - 1)}{2} e^{-2dh/(p\sqrt{wg})} \tag{21}$$

The concept of wave impedance is applied to define the equivalent impedance of an FSS structure. For an FSS, the equivalent impedance is given by (22) and corresponds to a parallel association between the FSS and input impedances. The representation through an equivalent impedance for the FSS structure is illustrated in Fig. 5(a) and the associated equivalent circuit in Fig. 5(b).

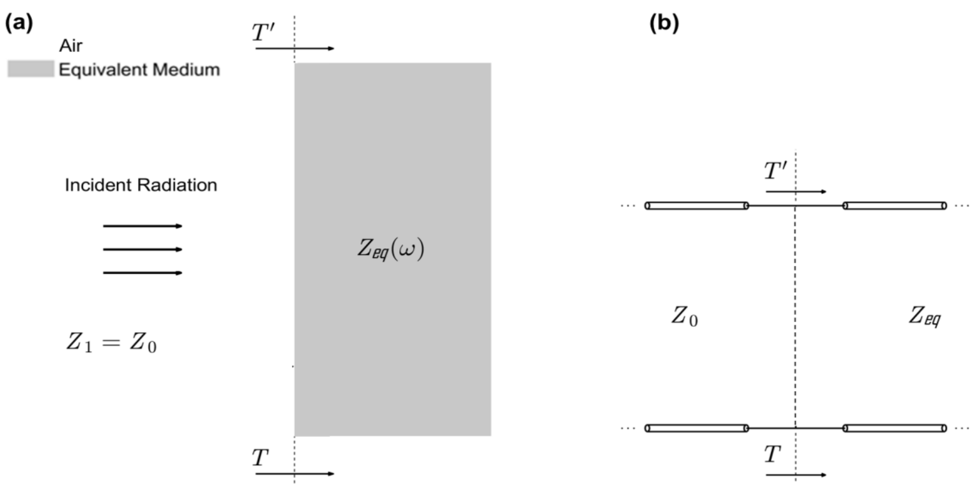

Fig. 5. FSS: (a) Representation in terms of equivalent impedance; (b) Associated equivalent circuit.

Brazilian Microwave and Optoelectronics Society-SBMO received 05 Dec 2023; for review 06 Feb 2024; accepted 16 May 2024
Brazilian Society of Electromagnetism-SBMag ISSN 2179-1074

The transmission and reflection coefficients are given in terms of the equivalent impedance of the FSS structure in (23) and (24), respectively.

$$Z_{eq}(\omega)=\frac{Z_{in}\cdot Z_{FSS}(\omega)}{Z_{in}+Z_{FSS}(\omega)} \tag{22}$$

$$T(\omega)=\frac{2Z_{eq}(\omega)}{Z_{eq}(\omega)+Z_0} \tag{23}$$

$$\Gamma(\omega)=\frac{Z_{eq}(\omega)-Z_0}{Z_{eq}(\omega)+Z_0} \tag{24}$$

For a freestanding FSS, the equivalent impedance is a parallel association between the FSS impedance and the free space characteristic wave impedance, $Z_{in}=Z_0$.

C. Equivalent Circuit Model - Wave Impedance

In the equivalent circuit models reported in the literature, for each type of FSS, the normalized immittance values of the equivalent circuit components associated with the FSS structure are obtained from the scaling of the Marcuvitz model. In particular, the geometric parameters of the periodic strip gratings (*w* and *g*) are scaled, as well as the function *F* given in (5), for oblique incidence, in (12), for normal incidence.

The equivalent circuit associated with an FSS square loop, in the configuration superimposed on a dielectric substrate, has a dielectric layer of thickness *h* and is represented by a line section of the same length. In the analysis of an FSS in the superimposed configuration with the equivalent wave impedance circuit model (ECM-WI), the approximation of transmission and reflection coefficients is calculated in five steps:

1- Dielectric substrate impedance, (25);

$$Z_d=\frac{Z_0}{\sqrt{\varepsilon_r[1-jtg(\delta)]}} \tag{25}$$

2- Input wave impedance, (26)-(28);

$$Z_{in}(\omega)=Z_0\frac{1+tanh(\gamma h)/\sqrt{\varepsilon_c}}{1+tanh(\gamma h)\cdot\sqrt{\varepsilon_c}} \tag{26}$$

$$\varepsilon_c=\varepsilon_r[1-jtg(\delta)] \tag{27}$$

$$\gamma=\frac{\pi\sqrt{\varepsilon_r}}{\lambda}[tg(\delta)+j2] \tag{28}$$

3- FSS impedance, (29)-(33);

$$Z_{FSS}(\omega)=R_{FSS}+jZ_0(X_L-1/B_C) \tag{29}$$

$$X_{TE}=X_{TM}=\omega L=\frac{d}{p}F(p,w,\lambda_{eff}) \tag{30}$$

$$B_{TE}=B_{TM}=\omega C=4\frac{d}{p}\varepsilon'_{ref}F(p,g,\lambda_{eff}) \tag{31}$$

$$\lambda_{eff}=\frac{c}{f\sqrt{\varepsilon_{eff}(\omega)}}=\lambda/Re\left\{\frac{1+tanh(\gamma h)\cdot\sqrt{\varepsilon_c}}{1+tanh(\gamma h)/\sqrt{\varepsilon_c}}\right\} \tag{32}$$

$$\varepsilon_{eff}(\omega) = Re\left\{\left(\frac{Z_0}{Z_{in}(\omega)}\right)^2\right\} \tag{33}$$

4- Expression (22) calculates the equivalent impedance;

5- The calculation of the transmission and reflection coefficients, given in (23) and (24).

In this model, according to (30) and (31), the Marcuvitz *F* function is scaled with the effective wavelength given by (32). For analysis of effective relative electric permittivity (ε_{ref}), the model for transmission lines of coplanar strips is adopted (CPS). From the analytical model of a CPS line, according to [21], the effective permittivity is given by (34), where: q_d is the filling factor given by (35); $K(\cdot)$ denotes the complete elliptic integral of the first type; where k, k', k_0, k'_0 are given as a function of the geometric parameters of the CPS line according to [22].

$$\varepsilon_{ref} = 1 + (\varepsilon_r - 1)q_d \tag{34}$$

$$q_d = \frac{1}{2}\frac{K(k')}{K(k)}\frac{K(k_0)}{K(k'_0)} \tag{35}$$

Table I lists the parameters for evaluating the effective permittivity as a function of the thickness of the dielectric layer. The results of the empirical formulas given in [9], [10] and [23], and through the CPS line model are compared, Fig. 6. It is observed that there is an agreement between the result [23] and the result of CPS line, in terms of asymptotic values, which bring promising initial validation to the model being worked on.

TABLE I. PARAMETERS USED IN SIMULATIONS OF EFFECTIVE ELETRIC PERMITTIVITY MODELS.

Model	**Resonance Frequency (GHz)**	**Physical Dimensions (mm)**				
		P	*d*	*w*	*g*	*N*
[9]	3.5	20	18	1.4	0.8	1.8
[10]						$\varepsilon_{ref} = \varepsilon_{rh} + (1-\varepsilon_{rh})e^{-2dh/(p\sqrt{wg})}$
[23]						0.8832

In relation to the empirical formulas, the effective permittivity values were lower using the CPS line model, Fig. 4.

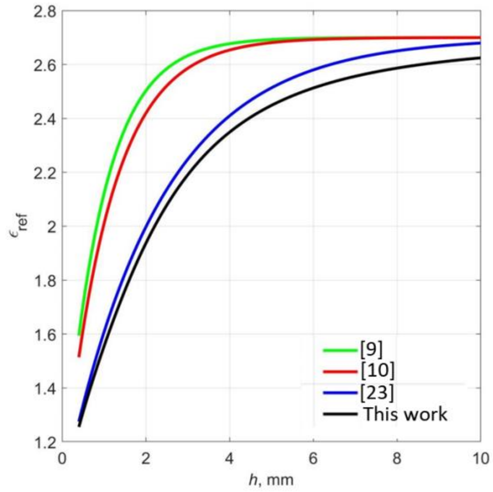

Fig. 6. Comparison between simulated results of effective electric permittivity models.

D. Equivalent Circuit Models

A comparative study of the approached models was carried out through computational simulations in Matlab® language. The following models were considered: equivalent circuit model (ECM) based on implementations available in [10], [14]; improved equivalent circuit model (iECM) with the effective permittivity, ε_{ref}, given in (34); equivalent wave impedance circuit model (ECM-WI) using the proposed adjustment of the effective permittivity (34), and the effective wavelength, λ_{eff} (32).

For the two proposed models, iECM and ECM-WI, the scaling of the Marcuvitz model for periodic strip gratings (q=2w or q= g) is carried out according to (36), whose values were optimized based on preliminary results of full wave simulation for superimposed square loop FSS. The reduction of the spacing parameter g in (36) considers the reduction of the effective permittivity calculated through (34) and, therefore, of the capacitive susceptance given by (19).

$$\begin{cases} q = 2.000.w \text{ and } q = 0.875 \cdot g, & \varepsilon_{ref} \approx 1 \\ q = 1.125 \cdot w \text{ and } q = 0.740 \cdot g, & c.c. \end{cases} \tag{36}$$

III. THEORETICAL AND EXPERIMENTAL RESULTS

A. Theoretical Results

Three square loop types FSS available in the literature with dielectric substrates made of polyester thin film and fiberglass (FR-4) were considered to obtain the values given in (36). Table II lists the geometric parameters of the addressed FSS including the considered dielectric materials.

TABLE II. PARAMETERS OF SQUARE LOOP TYPE FSS IN OVERLAPPED CONFIGURATION ON A DIELECTRIC.

FSS	**Reference**	**Material**	ε_r	**Geometrical Parameters (mm)**				
				p	*w*	*d*	*g*	*h*
1	[11]	Polyester	3.00	5.25	0.47	5.00	0.25	0.021
2	[24]	FR-4	4.40	42.50	2.00	31.95	10.55	1.60
3	[14]	FR-4	4.40	12.00	1.00	10.00	2.00	1.50

In order to compare the approximations of the implemented equivalent circuit models, the simulation results of the FSS transmission coefficients with the parameters listed in Table II are presented. The results of the proposed models (iECM and ECM-WI) are analyzed in relation to the results of the full-wave simulation (Ansoft Designer™), and the results available in the literature. The bandwidth was set at -10 dB allowing a wide useful range, corresponding to 90% of the reflected power.

FSS 1 obtained excellent agreement between the transmission coefficient results, Fig. 7(a). It was found that equivalent circuit models are well suited for FSS analysis on thin dielectric substrates, which have effective permittivity values close to those of air. FSS 2 presented an excellent result in the ECM-WI, both for resonance frequency (deviation of 0.44%) and for bandwidth (deviation of 1.72%). The ECM presented the largest deviations: 10.96% and 25.86%, respectively, Fig. 7(b). FSS 3 for the ECM-WI presented an excellent result among the models for resonance frequency (deviation of 0.62%). For bandwidth, iECM showed a smaller deviation of 4.21%, Fig. 7(c).

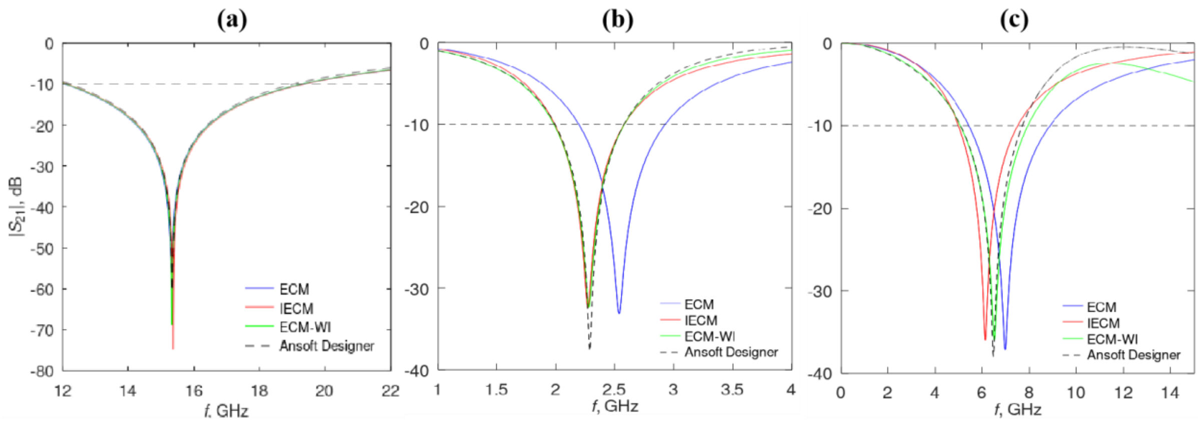

Fig. 7. Comparison between simulation results: (a) FSS 1; (b) FSS 2; (c) FSS 3.

The theoretical values for the resonance frequency and bandwidth parameters obtained for square loop FSS are listed in Tables III and IV, respectively. The deviations considered are calculated in relation to the results obtained using the Ansoft Designer™ simulation software.

TABLE IIII. NUMERICAL RESULTS OBTAINED FOR RESONANCE FREQUENCY.

FSS	Resonance Frequency (GHz)				Deviation (%)		
	ECM	**iECM**	**ECM-WI**	**Ansoft Designer™**	**ECM**	**iECM**	**ECM-WI**
1	15.31	15.36	15.32	15.33	0.13	0.20	0.07
2	2.53	2.26	2.27	2.28	10.96	0.88	0.44
3	6.96	6.12	6.50	6.46	7.74	5.26	0.62
				Mean Deviation (%)	6.28	2.11	0.38

TABLE IV. NUMERICAL RESULTS OBTAINED FOR BANDWIDTH.

FSS	Bandwidth (GHz)				Deviation (%)		
	ECM	**iECM**	**ECM-WI**	**Ansoft Designer™**	**ECM**	**iECM**	**ECM-WI**
1	7.27	7.26	7.22	6.84	6.29	6.14	5.56
2	0.73	0.58	0.59	0.58	25.86	0.00	1.72
3	3.43	2.50	2.85	2.61	31.42	4.21	9.20
				Mean Deviation (%)	21.19	3.45	5.49

B. ECM-WI Model Validation Results

An FSS prototype was built using the printed circuit manufacturing method, with a FR-4 substrate designed for a resonance frequency of 10 GHz, construction parameters indicated in Table V. An image of the manufactured prototype is presented in Fig. 8(a). The measured results were obtained with the aid of an acrylic base, a vector network analyzer model E5071C and two X-band horn antennas with a gain of 15 dB. The image of the assembled measuring arrangement is shown in Fig. 8(b).

TABLE V. PARAMETERS OF THE FSS PROTOTYPE ANALYZED.

Material	ε_r	P (mm)	w (mm)	d (mm)	g (mm)	h (mm)
FR-4	4.40	9.12	1.00	7.12	2.00	1.50

Brazilian Microwave and Optoelectronics Society-SBMO received 05 Dec 2023; for review 06 Feb 2024; accepted 16 May 2024
Brazilian Society of Electromagnetism-SBMag

ISSN 2179-1074

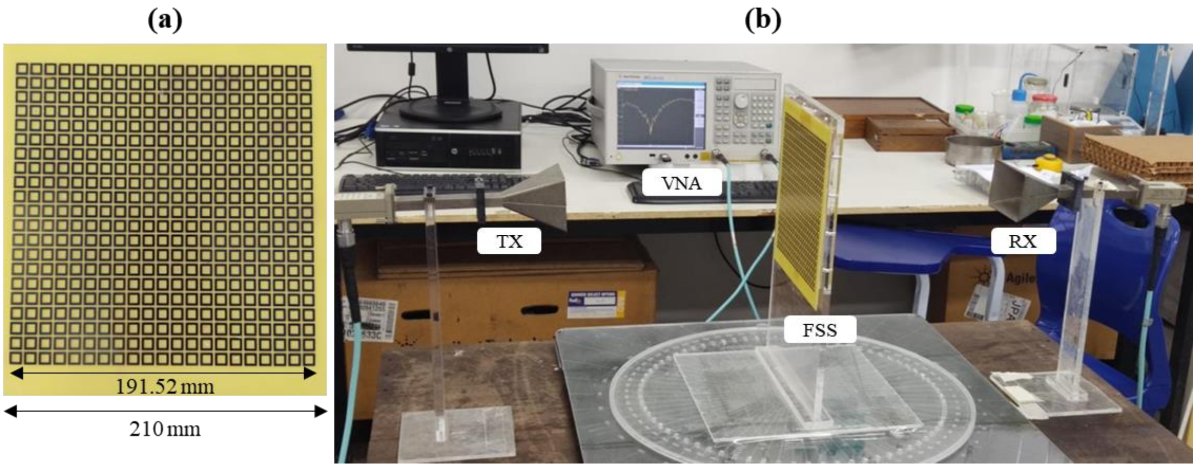

Fig. 8. Images: (a) Prototype; (b) Measurement arrangement.

In Fig. 9, the approximate analysis results (ECM and ECM-WI models) are compared with the Ansoft Designer™ results. There is excellent agreement between the ECM-WI model and the full-wave simulation for resonance frequency. In this case, the results of the ECM model were discrepant in relation to the full wave analysis, Fig. 9, proving the improvement introduced in the ECM-WI model.

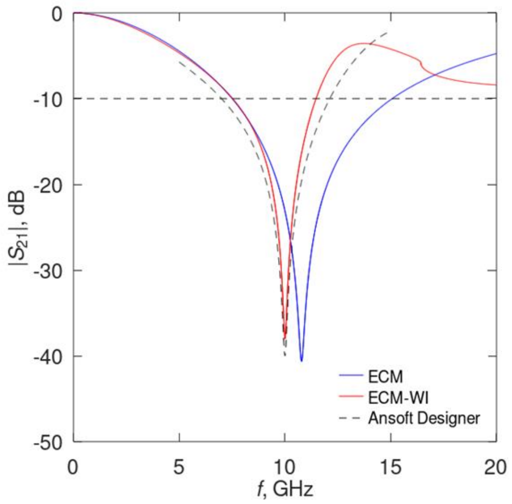

Fig. 9. Comparison between prototype simulation results.

From the comparative graph in Fig. 10, there is a good agreement between the simulated (ECM-WI and Ansoft Designer™) and measured results, both for the designed resonance frequency (10 GHz), with a deviation of 2.56%, as for bandwidth (3.94 GHz), with a deviation of 2.79% (between the ECM-WI model and the measured result).

When analyzing the results, it was possible to observe a discontinuity in Fig. 9, which corresponds to the grating lobe frequency ($p=\lambda_{eff}$) and determines the validity limit for the ECM-WI model. Regarding the measured results, the following deviations for resonance frequency (see Table VI) and bandwidth (see Table VII), in ECM-WI and Ansoft Designer™.

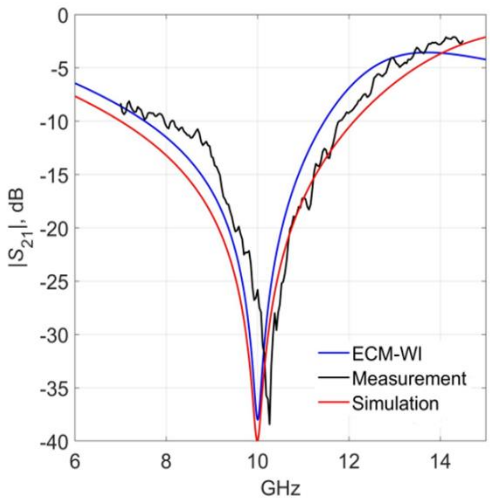

Fig. 10. Comparison between simulated and measured results of the prototype.

TABLE VI: NUMERICAL RESULTS OBTAINED FOR RESONANCE FREQUENCY.

RESONANCE FREQUENCY (GHz)			Deviation (%)	
ECM-WI	Ansoft Designer™	Measured	ECM-WI	Ansoft Designer™
10.00	10.00	10.26	2.56	2.56

TABLE VII: NUMERICAL RESULTS OBTAINED FOR BANDWIDTH.

Bandwidth (GHz)			Deviation (%)	
ECM-WI	Ansoft Designer™	Measured	ECM-WI	Ansoft Designer™
3.94	5.12	3.83	2.79	33.57

IV. CONCLUSION

A wave impedance equivalent circuit methodology for frequency selective surface analysis was presented. Two models, iECM and ECM-WI, were formulated for FSS structures with aligned periodic arrays of square loops, in the configuration superimposed on a lossy dielectric layer. Considering only the case of normal incidence, a contribution was made in the simplified formulation (12) and (13) for the Marcuvitz model. In this methodology, based on the FSS input impedance, an effective wavelength, expression (32), was calculated. The CPS line model, expression (51), was used to determine the effective permittivity of the FSS dielectric layer. Finally, to calculate the normalized immittances of the FSS equivalent circuit, the values of expressions (32), (34) and (36) were used to scale the Marcuvitz model, according to expressions (30) and (31).

To evaluate the performance of the ECM, iECM and ECM-WI models for normal incidence, four FSS were analyzed regarding transmission characteristics, functioning as band-reject filters. Considering the three theoretical results, the average deviations in absolute values were obtained for the ECM, iECM and ECM-WI models, respectively: i) in terms of resonance frequency: 6.28%, 2.11% and 0.38%; ii) in terms of bandwidth: 21.19%, 3.45% and 5.49%. These preliminary results indicated the effectiveness of the improvements proposed for the ECM, mainly in terms of bandwidth.

For the experimental results, deviation was obtained for the ECM-WI and Ansoft Designer™ model, respectively: i) in terms of resonance frequency: 2.56% and 2.56%; ii) in terms of bandwidth: 2.79%

  ISSN 2179-1074

and 33.57%. From these results, the developed ECM-WI model can be validated for normal incidence up to the resonance region.

ACKNOWLEDGMENT

This work was totally supported by the Federal Institute of Paraíba Graduate Program in Electrical Engineering (PPGEE-IFPB).

REFERENCES

[1] R. S. Anwar, L. Mao, H. Ning, "Frequency selective surfaces: a review," *Applied Sciences*, vol. 8, pp. 1689, 2018. DOI:10.3390/app8091689.

[2] R. Panwar, J. R. Lee, "Progress in frequency selective surface-based smart electromagnetic structures: a critical review," *Aerospace Science and Technology*, vol. 66, pp. 216-234, 2017. DOI:10.1016/J.AST.2017.03.006.

[3] N. Marcuvitz, "Waveguide Handbook," New York (USA), *McGraw Hill*, 1951.

[4] M. R. Chaharmir, J. Shaker, "Design of a multilayer x-/ka-band frequency-selective surface-backed reflectarray for satellite applications," in *IEEE Transactions on Antennas and Propagation*, vol. 63, pp. 1255-1262, 2015. DOI:10.1109/TAP.2015.2389838.

[5] N. Zabri, R. Cahill, A. Schuchinsky, "Polarisation independent resistively loaded frequency selective surface absorber with optimum oblique incidence performance," *IET Microwaves, Antennas & Propagation*, vol. 8, pp. 1198-1203, 2014. DOI:10.1049/iet-map.2014.0124.

[6] H. Zhou et al., "Filter-antenna consisting of conical FSS radome and monopole antenna," in *IEEE Transactions on Antennas and Propagation*, vol. 60, pp. 3040-3045, 2012. DOI:10.1109/TAP.2012.2194648.

[7] C. A. Balanis, "Modern Antenna Handbook," New York (USA): *Wiley*, 2008.

[8] F. Costa, A. Monorchio, G. Manara, "An equivalent circuit model of frequency selective surfaces embedded within dielectric layers," in *IEEE Antennas and Propagation Society International Symposium*, 2009. DOI:10.1109/APS.2009.5171774.

[9] F. Costa, A. Monorchio, G. Manara, "An overview of equivalent circuit modeling techniques of frequency selective surfaces and metasurfaces," in *Applied Computational Electromagnetics Journal*, vol. 29, pp. 960-976, 2014. DOI:10.1002/J.1538-7305.1975.TB03551.X.

[10] M. A. R. Barrera, W. P. Carpes, "Numerical Model of the Effective Permittivity for Square-Loop Frequency Selective Surfaces," in *IEEE Transactions on Magnetics*, vol. 51, pp. 1-4, 2015.

[11] R. J. Langley, E. A. Parker, "Equivalent circuit model for arrays of square loops," *Electronics Letters*, vol. 18, pp. 294-296, 1982. DOI:10.1049/EL:19820201.

[12] C. K. Lee, R. J. Langley, "Equivalent-circuit models for frequency-selective surfaces at oblique angles of incidence," in *IEE Proceedings H (Microwaves, Antennas and Propagation)*, vol. 132, pp. 395-399, 1985. DOI:10.1049/ip-h-2.1985.0070.

[13] A. L. P. S. Campos, A. G. Neto, E. P. Santos and M. W. B. Silva, "Proposed technique of analysis for absorber/transmitter frequency selective surfaces," in *Journal of Microwaves, Optoelectronics and Electromagnetic Applications*, vol. 20, 2021. DOI:10.1590/2179-10742021v20i21004.

[14] A. L. P. S. Campos, "Frequency Selective Surfaces: Analysis and Design," Superfícies Seletivas em Frequência: Análise e Projeto, *IFRN Editora*, vol. 1, pp. 196, 2009.

[15] D. Singh, A. Kumar, S. Meena, V. Agarwala, "Analysis of frequency selective surfaces for radar absorbing materials," *Progress In Electromagnetics Research B.*, vol. 38, pp. 297-314, 2012. DOI:10.2528/PIERB11121601.

[16] F. Costa, A. Monorchio, G. Manara, "Efficient analysis of frequency-selective surfaces by a simple equivalent-circuit model," in *IEEE Antennas and Propagation Magazine*, vol. 54, pp. 35-48, 2012.

[17] W. H. Jr. Hayt, J. A. Buck, "Engineering Electromagnetics," New York (USA), *McGraw Hill*, vol. 8, pp. 331-395, 2011.

[18] M. S. Nikoo, S. M-A. Hashemi, F. Farzaneh, "Theory of Terminated Nonlinear Transmission Lines," in *IEEE Transactions on Microwave Theory and Techniques*, vol. 66, pp. 91-99, 2018. DOI:10.1109/TMTT.2017.2731958.

[19] G. Bharti, K. Ranjan, G. Singh, "A synthesis technique of single square loop frequency selective surface at terahertz frequency," *Optik (Stuttgart)*, vol. 125, pp. 6428–6435, 2014. DOI:10.1016/J.IJLEO.2014.08.009.

[20] I. Anderson, "On the Theory of Self-Resonant Grids," in *Bell System Technical Journal*, vol. 54, pp. 1725-1731, 1975. DOI:10.1002/j.1538-7305.1975.tb03551.

[21] H. Berg, S. Gevorgian, "Line Capaciance and Impedance of Coplanar-Strip Waveguides on Substrates with Multiple Dielectric Layers," *2001 31st European Microwave Conference*, pp. 1-4, 2001. DOI:10.1109/EUMA.2001.339161.

[22] S. Butalla, "Calculation of the interstrip capacitance of the GE 2 / 1 GEM detector and measurement of theinterstrip capacitance of the GE 1 / 1-XS GEM detector," in *Content Management System Industry News*, pp. 1-7, 2018.

[23] G. L. R. Araújo, A. L. P. S. Campos, A. M. Martins, "Improvement of the equivalent circuit method for analysis of frequency selective surfaces using genetic algorithms and rational algebraic models," *Prog Electromagn Res Lett*, vol. 55, pp. 67–74, 2015. DOI:10.2528/PIERL15060803.

[24] T. Areias, R. Carvalho, A. L. P. S. Campos, A. G. Neto, J. J. G. Neto, M. M. Silva, "Frequency Selective Surface Microwave Absorber for WLAN Applications," in *Journal of Communication and Information Systems*, vol. 35, pp. 208-216, 2020. DOI:10.14209/jcis.2020.23.

